Facilitated Diffusion of the *Eco*RI DNA Methyltransferase Is Described by a Novel Mechanism†

Mark A. Surby and Norbert O. Reich*

Department of Chemistry, University of California, Santa Barbara, California 93106

Received August 10, 1995; Revised Manuscript Received December 11, 1995⊗

ABSTRACT: The contribution of nonspecific DNA to binding parameters (K_d, k_{off}, and k_{on}) was determined for the *Eco*RI DNA methyltransferase under noncatalytic conditions. An increase in DNA size from 14 to 775 base pairs causes a 20-fold decrease in K_d, while k_{off} remains constant over the same range. The calculated k_{on} increases with longer substrates, consistent with a facilitated diffusion mechanism. However, the combined results deviate from the model developed to describe facilitated diffusion [Berg, O.G., Winter, R. B., & von Hippel, P. H. (1981) *Biochemistry 20*, 6929−6948]. Our results were successfully simulated using numerical integration of a kinetic scheme invoking protein dissociation via the ends of DNA. Consistent with this scheme, the methyltransferase dissociates more slowly from a circularized DNA molecule than from the identical linearized form. The simulation strategy correctly models our data with the methyltransferase and should be generally useful for routine modeling of facilitated diffusion involving protein−DNA systems.

Sequence-specific DNA recognition by proteins is a fundamental biological process. A full understanding of the underlying mechanisms of interaction requires information regarding the kinetic parameters that govern protein binding to a specific DNA site (von Hippel, 1994). However, the polymeric nature of DNA complicates such mechanistic studies. For example, a protein's occupancy at a specific site is modulated by the length of flanking, nonspecific DNA and the protein's affinity for such sequences (von Hippel & Berg, 1986). Additionally, the presence of nonspecific DNA can increase a protein's affinity for the DNA substrate as a whole and allow for association with its specific site at a rate faster than the limit set by three-dimensional diffusion (Riggs et al., 1970; Winter & von Hippel, 1981). This has been attributed to facilitated diffusion to the specific site via interactions with nonspecific flanking DNA. In essence, the protein targets the entire DNA molecule for binding and then locates the specific site by sliding, hopping, or intersegment transfer (for a review see von Hippel and Berg, 1989). Facilitated diffusion has been proposed for a variety of proteins including *Eco*RI endonuclease (Jack et al., 1982), RNA polymerase (Ricchetti et al., 1988) *Bam*HI endonuclease (Nardone et al., 1986), T4 endonuclease V (Dowd & Lloyd, 1990), and the T4 late enhancer complex (Herendeen et al., 1992).

*Eco*RI DNA methyltransferase (MTase)[1] is a component of a type II restriction−modification system and methylates the central adenine of the double stranded recognition sequence 5′-GAATTC-3′. Our previous characterization of the DNA length dependency of the catalytic constants of the MTase (M. A. Surby and N. O. Reich, accompanying manuscript) shows that facilitated diffusion makes a significant contribution to the enzyme's overall catalytic efficiency. We sought to compare our results with a detailed kinetic model of facilitated diffusion which relates DNA length to thermodynamic (K_d) and kinetic (k_{off} and k_{on}) binding constants (Berg et al., 1981). The MTase catalytic cycle was therefore limited to events up to and including specific site binding. Sinefungin, an analog of the methyl-donating cofactor *S*-adenosylmethionine (AdoMet), stabilizes an inactive ternary complex (MTase−DNA−sinefungin) (Reich & Mashhoon, 1990) and was used to determine K_d and k_{off} for DNA substrates of varying lengths. We compare our findings with those determined under catalytic conditions (Surby and Reich, accompanying manuscript), the results obtained for the *Eco*RI endonuclease (Jack et al., 1982), and data calculated using a theoretical model of facilitated diffusion (Berg et al., 1981). Inconsistencies between the theory and the results reported in this paper are reconciled by an extension of the original theory, and this modification is then tested experimentally.

MATERIALS AND METHODS

Materials. *Eco*RI MTase was purified from *Escherichia coli* strain MM294 harboring plasmid pPG440 (Greene et al., 1978). Phosphoramidites and ancillary DNA synthesis reagents were obtained from Milligen/Biosearch. [γ-^{32}P]ATP (6000 Ci/mmol) was purchased from Amersham. *Bam*HI, *Hin*dIII, and *Eco*RV endonucleases and calf intestinal alkaline phosphatase were purchased from Promega. *Dde*I and *Xmn*I endonuclease and T4 polynucleotide kinase were from New England Biolabs.

DNA Substrates. DNA substrates ranging in size from 14 to 775 base pairs (bp) were used. The 14 bp and 32 bp substrates that have the sequence 5′-GGCGGAATTCGCGG-3′ and 5′-ACGATCAGACACGGAATTCGCGACGAT-CAGCT-3′, respectively, were synthesized on a Biosearch 3810 DNA synthesizer using β-cyanoethyl phosphoramidites and purified by C_{18} reverse-phase HPLC (Becker et al.,

† This work was supported by grants from the National Science Foundation (MCB-9018474) and the Amercian Cancer Society (JFRA-332) to N.O.R.

* To whom correspondence should be addressed.

⊗ Abstract published in *Advance ACS Abstracts,* February 1, 1996.

[1] Abbreviations: MTase, methyltransferase, bp, base pairs; AdoMet, *S*-adenosylmethionine; ENase, endonuclease.

0006-2960/96/0435-2209$12.00/0

1985). The concentrations of single strands were determined spectrophotometrically. Complementary single strands were annealed, and confirmation of the double-stranded form was through autoradiography with nondenaturing polyacrylamide gel electrophoresis. The larger substrates were generated from plasmid pBR322 using the following restriction digests: 101 bp, *Dde*I and *Hin*dIII; 378 bp, *Eco*RV and *Ssp*I; and 775 bp, *Bam*HI and *Xmn*I. All substrates were designed to keep the *Eco*RI site as centrally located on the substrate as possible. Plasmids pBR322 and pBR322(ΔRI) were isolated from *E. coli* strain MM294 by alkaline lysis and purified using QIAGEN maxi-prep columns, and their concentrations determined spectrophotometrically. Plasmid pBR322(ΔRI) is a modified version of pBR322 from which the *Eco*RI site was removed (M. A. Surby and N. O. Reich, accompanying manuscript). Restriction digests were performed using the suppliers' recommended buffers supplemented with 200 μg of BSAmL. Double digests were performed in the buffer that optimized the activity of both enzymes. Endonucleases were heat inactivated, and the desired fragment was isolated using a Waters GenPak FAX HPLC column (Stowers et al., 1988).

The off-rate kinetics of the MTase from circular versus linear DNA substrates of the same length were determined with plasmid pSP72 (Promega)-derived sequences. The segment from position 2281 to 187 on the 2462 bp plasmid was PCR amplified (Innis & Gelfand, 1990), resulting in a DNA fragment of 368 bp containing a single *Eco*RI site located 120 bp from the nearest end. The fragment was purified by gel excision and extensive ethanol precipitation, ^{32}P labeled, and ligated under conditions of very dilute DNA which resulted in approximately 50% conversion of linear to circular with no multimeric linear species present.

Thermodynamic Dissociation Constant Determinations. DNA substrates were radiolabeled with ^{32}P using T4 polynucleotide kinase and [γ-^{32}P]ATP after removal of the 5′-phosphates using calf intestinal alkaline phosphatase. Excess ATP was removed using Bio-Spin 6 columns (Bio-Rad) after the kinase reaction cocktail had been diluted 10-fold in 10 mM Tris, pH 8.0, 1.0 mM EDTA, and 100 mM NaCl. Thermodynamic dissociation constant (K_d) were determined as previously described (Reich et al., 1992). The binding cocktails contained DNA, 100 mM Tris, pH 8.0, 10 mM EDTA, 200 μg of BSA/mL, 10 mM DTT, 20 μM sinefungin, and various MTase concentrations. DNA concentrations were kept below the expected K_d for each substrate. The ionic strength of the assay mixture was determined to be 0.05 by comparison of the conductivity with a standard curve using solutions of known NaCl concentration. The reactions were incubated at 37 °C for 20 min, combined with loading buffer (final concentrations of 6.5% glycerol, 7 mM Tris-borate, 0.2 mM EDTA), and loaded onto a polyacrylamide gel of appropriate concentration (wt/vol): 12% for 14 and 32 bp, 10% for 101 bp, 8% for 378 bp, and 6% for 775 bp. Gel electrophoresis was performed at 4 °C to eliminate ternary complex dissociation during migration. The gels were run at 500 V for 5 min and then at 300 V for 2 h, dried ont Whatman 3MM filter paper, and exposed to X-ray film (Fuji AIF RX) with an intensifying screen at −70 °C. The exposed film was scanned with an LKB Ultroscan XL laser densitometer to determine the relative amounts of ternary complex formed at each enzyme concentration. The dissociation constants were determined by fitting this data to a standard hyperbolic binding expression. K_d's are the result of at least three determinations and the error reported as the standard deviation from the mean.

The dissociation constant for nonspecific DNA was determined indirectly using a modified version of the gel shift assay described above. The MTase was held at a constant concentration of 1 nM and allowed to equilibrate with approximately 0.4 nM radiolabeled 14 bp DNA and an increasing concentration of unlabeled pBR322(ΔRI) (0−5 nM). All other assay conditions remained the same. The autoradiograms were scanned to determine the concentration of complexed 14mer ([ES]) with increasing plasmid concentrations ($[\Delta RI]_0$). The dissociation constant for the plasmid was then determined using a modification of a method developed to analyze competitive ligand binding to a receptor (van Zoelen, 1992). The following equation was used to fit the experimental data, [ES] vs $[\Delta RI]_0$, to determine the nonspecific dissociation constant (K_{ns}) when the specific dissociation constant (K_s) and the initial and free concentrations of 14 bp DNA ($[S]_0$ and [S], respectively) are known:

$$[ES] = \frac{[S]_0[S]}{K_s + [S] + K_s[\Delta RI]/K_{ns}} \quad (1)$$

The concentration of free inhibitor ([Δ*RI*]) in eq 1 was determined using the following:

$$[\Delta RI] = [\Delta RI]_0 \Big/ \left(1 - \frac{K_s}{K_{ns}} + \frac{[S]_0 K_s}{[S]K_{ns}}\right) \quad (2)$$

Determination of k_{off}. The kinetic dissociation constant of the MTase with the various DNA substrates was determined by adding an excess of unlabeled competitor DNA to a preequilibrated mixture of the MTase and the substrate of interest and monitoring the decrease in labeled ternary complex over time. The labeled substrate DNA was preincubated with the MTase as described above for the equilibrium constant. DNA concentrations were approximately equal to their K_d (0.02−0.4 nM) while the MTase concentration was 2−5 times the K_d value (0.04−2 nM). Unlabeled pBR322 was added to the reaction mix to a final concentration of 40 nM. Control experiments in which the unlabeled competitor DNA was added prior to labeled substrate resulted in no detectable complex formation, showing that the competitor was an effective trap at these concentrations. Aliquots were then removed, mixed with loading buffer, and loaded onto a polyacrylamide gel that was running at 500 V at 4 °C. The shortest reproducible time between sample applications possible with this method was 20 s. After the last sample was loaded, the running voltage was reduced to 300 V and the gel was run for 2 h. The gel was then dried, exposed to film, and the autoradiogram scanned to determine the relative amounts of ternary complex remaining at the various time points. The data was plotted as the natural logarithm of (AUC) vs time, where AUC is the integrated densitometric area associated with the ternary complex in a given lane. The negative slope of this linear plot is the kinetic dissociation constant, k_{off}, whose unit is s^{-1}.

RESULTS

Increasing DNA Length from 14 to 775 bp Results in a 20-Fold Decrease in K_d. A gel shift assay was used to

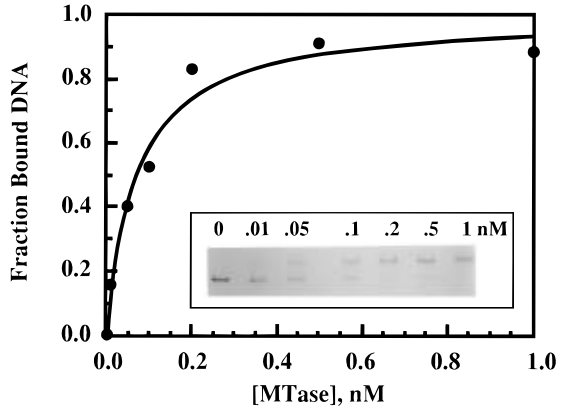

FIGURE 1: Binding curve for MTase−378 bp DNA−sinefungin complex. Densitometric data obtained from the upper bands of the gel shift autoradiogram shown in the inset was plotted versus the corresponding MTase concentration and was fit to a standard bimolecular binding curve. The best fit yielded an equilibrium dissociation constant of 0.07 nM. (Inset) Autoradiogram of gel shift assay for binding of MTase to the 378 bp DNA at 37 °C. Varying MTase concentrations were incubated with approximately 0.01 nM radiolabeled 378 bp NDA, 20 μM sinefungin, 100 mM Tris pH 8.0, 10 mM EDTA, 10 mM DTT, and 200 mg of BSA/mL for 20 min at 37 °C before being run on an 8% polyacrylamide gel at 4 °C. The autoradiogram shows an increase in the amount of MTase−DNA−sinefungin complex (upper bands) and a corresponding decrease in the amount of free 378 bp DNA (lower bands) as the MTase concentration is increased.

examine the DNA length dependence of the K_d of the MTase (Reich et al., 1992). An autoradiogram of a typical experiment is shown in Figure 1A. The 378 bp DNA was incubated with increasing MTase concentrations and saturating sinefungin (Reich et al., 1992). The binding isotherm derived from the densitometric scanning of the ternary complex band from this experiment is shown in Figure 1B. DNA concentrations were at least 10-fold lower than the enzyme concentrations used in each experiment to ensure that true K_d values were being determined. The results of all K_d determinations can be seen in Table 1. There is a distinct DNA length dependence associated with K_d, with a 20-fold decrease observed between the 14 bp and 775 bp substrates.

Increasing DNA Length Has No Effect on k_{off}. An autoradiogram of a typical determination of the k_{off} for the 14mer is shown in Figure 2A. Initial concentrations of MTase and DNA were chosen to maximize the amount of ternary complex in the preincubation mixture while remaining well below the concentration of the unlabeled competitor DNA. The concentration of competitor DNA was chosen so that there was no change in the observed k_{off} with further increases in DNA concentration (data not shown). The relative amount of ternary complex remaining at a given time was determined by densitometric scanning of the upper band and plotted as shown in Figure 2B. Unlike the thermodynamic dissociation constant, the kinetic dissociation constant appears to have little to no dependency on the DNA length (see Table 1). A similar lack of length dependency was observed when the k_{off} determinations were made at room temperature rather than at 37 °C in order to determine if slowing down the dissociation process would reveal a trend that was hidden at the higher temperature (data not shown). The kinetic association constant (k_{on}) for a given substrate was calculated from the observed K_d and k_{off}. As shown in Table 1, k_{on} increases with increasing length, which is characteristic of facilitated diffusion [Berg et al. (1981) and Winter et al. (1981)].

K_d of Nonspecific DNA is 0.35 μM. The average affinity of the MTase for a nonspecific site was determined in order to accurately model the effects of nonspecific DNA on the apparent binding constant of a given substrate. This was accomplished by obtaining K_{ns} for a plasmid which contained no *Eco*RI sites [pBR322(ΔRI)] and then multiplying this value by the number of nonspecific sites on the substrate, which, in the case of a large substrate, is approximately equal to the number of base pairs [4360 for pBR322(ΔRI)]. The autoradiogram used for this experiment and the fit to eqs 1 and 2 can be seen in Figure 3. The value of K_{ns} determined from the fit was 0.081 nM, which corresponds to a K_d of 3.5×10^{-7} M per nonspecific site.

Comparison of K_d, k_{on}, and k_{off} Length Dependencies with the Theory of Berg et al. (1981). An attempt was made to utilize the rate equations describing k_{off} and k_{on} in terms of facilitated diffusion developed by Berg et al. (1981) to fit the experimental data shown in Table 1. The following equations were used for this analysis:

$$k_{on} = 2Sk_{assoc} \tanh[L(2S)^{-1}] \quad (3)$$

and

$$k_{off} = \frac{k_{assoc}}{K_s(2S)^{-1} \coth[L(2S)^{-1}] + K_{ns}} \quad (4)$$

where k_{assoc} is the intradomain nonspecific association rate constant, S is the average number of base pairs that the protein scans prior to dissociation, L is the length of the DNA substrate in DNA base pairs, K_s is the equilibrium constant for specific association, and K_{ns} is the equilibrium constant for nonspecific dissociation (Berg et al., 1981). Our k_{on} data were successfully fitted using eq 3, resulting in values of $k_{assoc} = 2.4 \times 10^6$ M^{-1} s^{-1} and $S = 141$ bp. However, using these same values in eq 4 results in k_{off} increasing from 0.013 to 0.20 s^{-1} and K_d decreasing from 0.39 to 0.30 nM as the DNA length is increased from 14 to 775 bp, respectively. These results are clearly in conflict with the data presented in Table 1, where k_{off} is relatively independent of DNA length and K_d decreases 20-fold as the DNA length is increased from 14 to 775 bp. One of the explicit assumptions in the theory is that DNA molecules are sufficiently long such that protein−DNA interactions at the ends of the DNA would be unimportant (Berg et al., 1981). However, as the DNA length gets smaller, the probability of an encounter with either end of the DNA molecule during the sliding phase increases and the potential outcome of such an event must be considered. One logical consequence of encountering a DNA end is the loss of substantial binding potential resulting in decreased binding stability. The magnitude of this effect could be protein specific, with a protein which is stable at the end remaining on the DNA and agreeing with the theory, while proteins with low end stability, such as might be the case with the MTase, dissociating from the end and showing deviations. An alternative reason for a k_{off} that is relatively independent of length would be that the MTase dissociates directly from the specific site into solution without going through a nonspecific DNA bound intermediate.

Smaller k_{off} for Circular DNA Confirms the End Dissociation Hypothesis. In order to test whether the relative

Table 1: Thermodynamic and Kinetic Constants Obtained for DNA Substrates of Varying Length[a]

substrate length	K_d (nM)		k_{off} (s^{-1})		$10^{-8} \times k_{on}$ (M^{-1} s^{-1})	
	exp	sim	exp	sim	exp	sim
14 bp	0.43 ± 0.08	0.41 ± 0.09	0.019 ± 0.006	0.013 ± 0.002	0.42 ± 0.15	0.32 ± 0.02
32 bp	0.29 ± 0.05	0.22 ± 0.05	0.017 ± 0.005	0.014 ± 0.002	0.59 ± 0.21	0.65 ± 0.03
101 bp	0.10 ± 0.02	0.10 ± 0.02	0.016 ± 0.005	0.016 ± 0.002	1.6 ± 0.6	1.6 ± 0.04
378 bp	0.07 ± 0.01	0.05 ± 0.02	0.018 ± 0.005	0.017 ± 0.003	2.6 ± 0.9	3.8 ± 0.5
775 bp	0.02 ± 0.01	0.04 ± 0.02	0.017 ± 0.005	0.020 ± 0.004	8.5 ± 3	4.8 ± 0.8

[a] Numbers under "exp" are the result of at least three determinations using a gel shift assay and are shown ± 1 SD. The values under "sim" were generated using KINSIM, Scheme 1, and the rate constants listed in Table 2. The values following "±" represent the limits of possible values for the simulated constants using the ranges listed in Table 2.

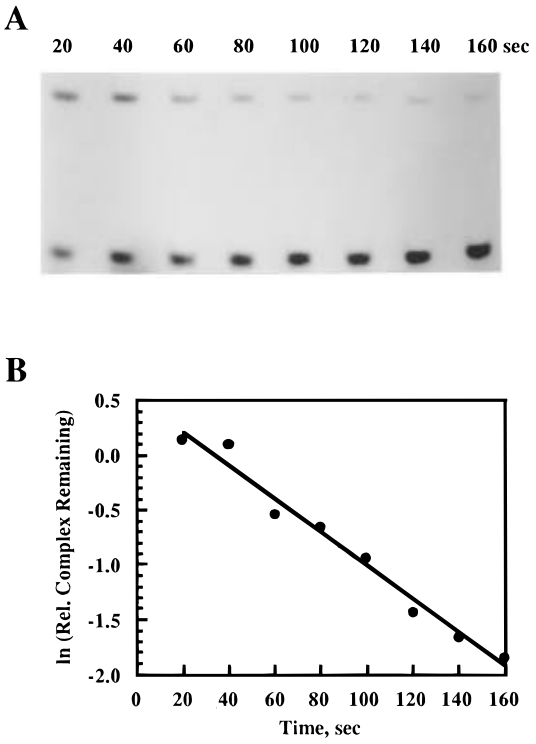

FIGURE 2: Gel shift assay for k_{off} determinations. (A) Autoradiogram of gel shift assay for kinetic dissociation constant of the MTase from the 14 bp DNA at 37 °C. Approximately 0.5 nM radiolabeled 14 bp DNA and 1 nM MTase were preincubated in the binding cocktail described in the legend for Figure 1A for 20 min at 37 °C. Unlabeled plasmid pBR322 was then added to a final concentration of 40 nM. Aliquots were removed at the indicated times and were loaded onto a 12% polyacrylamide gel running at 4 °C. The autoradiogram shows a decrease in the MTase−DNA−sinefungin complex (upper bands) and a corresponding increase in the amount of free 14 bp DNA (lower bands) as the time of incubation with the competitor DNA increases. (B) Plot to determine the kinetic dissociation constant of the MTase from the 14 bp DNA. The natural logarithm of the densitometric data obtained from the upper bands of the gel shift assay in panel A was plotted versus time and a linear fit was applied. The best fit yielded a first-order kinetic dissociation constant of 0.015 s^{-1}.

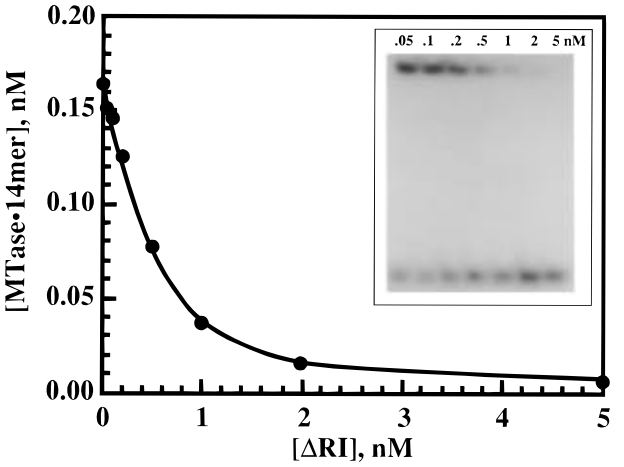

FIGURE 3: Binding curve for nonspecific DNA competition assay with the 14 bp DNA. The equilibrium dissociation constant for a nonspecific DNA site was determined using densitometry measurements of the upper band from the autoradiogram (inset). Equations 1 and 2 were used to generate the curve through the data points and to determine the dissociation constant for the plasmid. This was then multiplied by the number of nonspecific sites on the plasmid (4360) to approximate the average dissociation constant per nonspecific site. (Inset) Autoradiogram of nonspecific DNA competition assay was the 14 bp DNA at 37 °C. The equilibrium dissociation constant for a nonspecific site was determined indirectly using a modified gel shift assay in which 1 nM MTase and 0.16 nM radiolabeled 14 bp DNA was incubated with increasing concentrations of unlabeled plasmid pBR322(ΔRI) for 20 min at 37 °C. The amount of MTase−DNA−sinefungin complex (upper bands) decreases and the corresponding amount of free 14 bp DNA (lower bands) increases as the initial concentration of pBR322-(ΔRI) is increased, competing with the radiolabeled 14 bp DNA to form the unlabeled MTase−plasmid−sinefungin complex.

independence of k_{off} is due to dissociation via DNA ends or direct dissociation from the specific site, the k_{off} of the MTase from both a circular and a linear DNA substrate of equivalent length were compared. The predicted results were that the two substrates would have equivalent values of k_{off} if dissociation was directly from the specific site, while circular DNA—having no ends—would have a lower k_{off} than the linear substrate if end dissociation was occurring. Circular DNA was prepared by ligation of a ^{32}P-labeled 368 bp linear DNA fragment under very dilute conditions, resulting in cyclization in the absence of multimer formation. Identity of the circular form was confirmed by restriction analysis.

The dissociation of the MTase from both substrates was performed in the same tube so that the k_{off} from each substrate could be directly compared and complications from sample variation would be minimized. The circular DNA migrated much more slowly than the linear substrate, making it necessary to use a 3.5% polyacrylamide gel in order to get adequate resolution of the various bands on the same gel. As can be seen in Figure 4, the dissociation of the MTase from the circular DNA is noticeably slower than that from linear DNA. Determination of the kinetic dissociation constant from three separate experiments results in a k_{off} of 0.019 s^{-1} for linear DNA and 0.006 s^{-1} for circular DNA. Thus, removal of the DNA ends results in a 3-fold decrease in k_{off}.

Fitting the Experimental Results to a Kinetic Scheme Incorporating End Dissociation. In order to test whether a mechanism of facilitated diffusion involving dissociation via DNA ends would fit the experimental results shown in Table 1, two steps were added to the kinetic scheme of facilitated

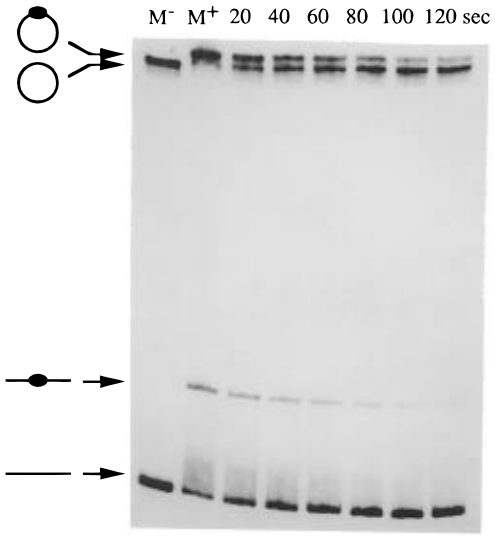

FIGURE 4: Autoradiogram used to determine k_{off} of the MTase from both circular and linear DNA of the same length. M^- and M^+ are controls which correspond to labeled 368 bp DNA that is either unbound or bound by the MTase, respectively, in the absence of any added unlabeled competitor DNA. The numbers are the time, in seconds, between addition of competitor DNA and loading of the sample on the gel. The schematic to the left of the autoradiogram identifies the bands corresponding to the individual DNA species: linear, unbound; linear, bound; circular, unbound; and circular, bound.

Scheme 1

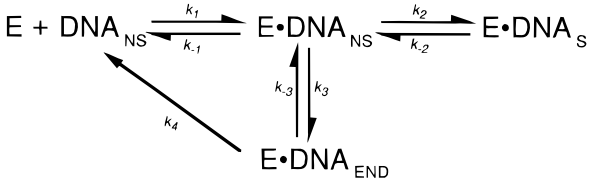

diffusion developed by Berg et al. (1981): (1) linear diffusion to and from the DNA end to nonspecific DNA and (2) dissociation from the end of the DNA molecule into free solution (see Scheme 1). Numerical integration of this kinetic scheme was then performed using the computer program, KINSIM (Barshop et al., 1983), which has been used in many studies which involve complex kinetic mechanisms (Kati et al., 1992; Polesky et al., 1992; Brown et al., 1994; Moore & Lohman, 1994). One advantage of the method of computer numerical integration is that no simplifying assumptions regarding the reaction conditions needed to be made; any combination of enzyme and substrate concentrations may be simulated using this technique. In addition, this program is very flexible in its ability to incorporate and test new hypotheses as dictated by unusual experimental results. The method requires reasonable estimates to be made for the microscopic rate constants that describe a particular system. This was done for Scheme 1 and the rationale for each of our estimates is described in the following paragraphs. The assumptions used to determine the initial values of the microscopic rate constants were simply an attempt to obtain reasonable starting values for our simulations rather than absolute determinants of these constants. A range of values around these initial estimates was tested for those that best fit the experimental data.

Rationale and Definition of Rate Constants.

k_1. This is the rate constant for the association of a protein with nonspecific DNA. The Debye−Smoluchowski equation was used as a reasonable estimate of this parameter (von Hippel & Berg, 1989):

$$k_1 = 4\pi\kappa af(D_{prot} + D_{dna})N_0/1000 \quad (5)$$

where κ is a unitless steric interaction factor, a is the interaction radius (in cm), f is a unitless electrostatic factor, D_{prot} and D_{dna} are diffusion constants for the MTase and DNA molecule, respectively (in cm^2/s), and N_0 is Avagadro's number. Since a facilitated diffusion mechanism allows for initial association with the entire DNA molecule, the radius of gyration (R_g) of the DNA was used as an estimate a and R_g was defined in terms of the worm-like coil model (Bloomfield et al., 1974):

$$R_g = \sqrt{\frac{bL}{3}\left[1 - \frac{b}{L} + \frac{b}{L}\exp\left(-\frac{L}{b}\right)\right]} \quad (6)$$

where b is the persistence length of DNA (assumed here to be 5×10^{-6} cm) and L is the length of the DNA (3.4×10^{-8} cm $\times$ bp). While a rigid rod model may be more appropriate for the shorter DNA substrates investigated here, evaluation of the two models showed very little deviation with lengths of 14 and 32 bp (data not shown). Therefore, the worm-like coil model sufficed for an initial estimate of k_1. D_{prot} was estimated using the Svedberg equation:

$$D = \frac{RTs}{M(1 - \upsilon\rho)} \quad (7)$$

where R is the gas constant, T is the temperature (in Kelvin), s is the sedimentation coefficient, M is the molecular weight, υ is the partial specific volume, and ρ is the density of water. The published values of s, M, and υ for the MTase (Rubin & Modrich, 1977) were used for D_{prot} and resulted in a value of 8×10^{-7} cm^2/s. Since D_{dna} is generally considered to be $<10^{-8}$ cm^2/s (von Hippel & Berg, 1989), this term will not contribute to k_1. κ was estimated to be 1/20, which assumes that $^1/_5$ of the DNA surface and $^1/_4$ of the MTase surface represent proper complex forming orientations (von Hippel and Berg, 1989). f was set at unity since the electrostatic interaction between the MTase and DNA is uncharacterized.

k_{-1}. This is the dissociation rate constant for the protein from nonspecific DNA. Experimental values for both the thermodynamic binding constant for nonspecific DNA (K_{ns}) and the kinetic association constant (k_{on}) for a small (14 bp) DNA molecule were determined. Assuming that k_{on} for a nonspecific site will be similar to that for the 14 bp DNA, k_{-1} can be approximated by multiplying the corresponding k_{on} by K_{ns}.

k_2. This is the association rate constant for the protein using facilitated diffusion to move from nonspecific DNA to the specific DNA-binding site. The expression for facilitated diffusion by sliding developed by Berg et al. (1981) was used to describe this step:

$$k_2 = \frac{k_{-1}}{[[L(2S)^{-1}\coth[L(2S)^{-1}]] - 1]} \quad (8)$$

where L is the length of the DNA substrate in base pairs and S is the average number of base pairs that the protein scans prior to dissociation. An initial value of $s = 200$ bp was based on the trends observed here and in the catalytic

Table 2: Final Values of Microscopic Rate Constants Derived from Computer Simulations of Scheme 1[a]

DNA length	$10^{-8} \times k_1$ (M^{-1} s^{-1})	k_{-1} (s^{-1})	k_2 (s^{-1})	k_{-2} (s^{-1})	k_3 (s^{-1})	k_{-3} (s^{-1})	$10^{-5} \times k_4$ (s^{-1})
14 bp	0.6 ± 0.1	8 ± 4	31000 ± 5000	0.033 ± 0.004	31000 ± 5000	120000 ± 20000	2.5 ± 0.5
32 bp	1.3 ± 0.2	8 ± 4	5900 ± 900	0.033 ± 0.004	5900 ± 900	76000 ± 12000	2.5 ± 0.5
101 bp	3.7 ± 0.4	8 ± 4	590 ± 90	0.033 ± 0.004	590 ± 90	28000 ± 4000	2.5 ± 0.5
378 bp	11.0 ± 1.5	8 ± 4	43 ± 6	0.033 ± 0.004	43 ± 6	8100 ± 1200	2.5 ± 0.5
775 bp	17.8 ± 2.1	8 ± 4	11 ± 2	0.033 ± 0.004	11 ± 2	4400 ± 600	2.5 ± 0.5

[a] The listed values are those which generated the best fit to the experimental values of K_d, k_{off}, and k_{on} using KINSIM and the kinetic mechanism shown in Scheme 1. The $\pm$ numbers represent the range of values for each constant that result in less than 15%−20% variation in the simulated values of K_d, k_{off}, and k_{on} listed in Table 1.

studies (M. A. Surby and N. O. Reich, accompanying manuscript).

k_{-2}. This is the dissociation rate constant for the protein moving from the specific DNA site to nonspecific DNA. This was approximated by the k_{off} that was measured for the longest DNA substrate (775 bp). Contributions from a destabilizing end association (k_3) or a stabilizing specific site reassociation (k_2) to k_{off} should be small for a long DNA substrate, making k_{-2} rate limiting for k_{off}.[2]

k_3. This is the association rate constant for the movement of the protein from nonspecific DNA to the end of the DNA substrate. For the kinetic scheme presented here, the end of the DNA is defined as the last nonspecific site at the terminus of the molecule for which all normal contacts are maintained. On the average, a protein bound to nonspecific DNA will have an equal probability for sliding to either the end of the substrate or to the specific site for a linear DNA substrate with a single specific binding site. Therefore, the expression for k_2 was used for k_3 as well. This seems especially valid given the general nature of the expression: there are no terms associated with either specific site or end bound protein.

k_{-3}. This is the dissociation rate constant for movement of the protein from the unique nonspecific site at the end of the DNA molecule to the generic population of nonspecific DNA. Since all normal nonspecific contacts are assumed to be maintained at the terminal nonspecific site, this is again merely a sliding process and can be described by the expression for k_2. However, this expression was multiplied by half the length of the DNA molecule to reflect the average number of nonspecific sites available to dissociate to before reaching the specific site.

k_4. This is the dissociation rate constant for the protein coming off the end of the DNA molecule into solution. This constant incorporates all steps for which nonspecific contacts are lost as the protein slides off the DNA and changes in the value of this constant reflect the probability of dissociation if even a single base pair's worth of nonspecific interactions are removed. A reasonable lower limit for k_4 is k_{-1}, which would assume that the stability at the end of the DNA is no different than any other nonspecific site. In order to determine the upper limit of k_4, one must assume that the activation energy required to dissociate from a DNA end is equal to the binding energy for a nonspecific site.[3] Given that $K_{ns} = 3.5 \times 10^{-7}$ M, the maximal value of k_4 is 2.3×10^6 s^{-1}. There is no expression for protein associating with a DNA end (k_{-4}) in our model since it is much more likely that the protein will associate with the DNA via the pathway described for k_1.

Kinetic Simulations. Individual kinetic simulations were run for each substrate in order to determine the best fit values of the kinetic constants that determine k_{on}, k_{off}, and K_d. For k_{on} simulations, k_{-2} was set at zero and the appearance of $E{\cdot}DNA_s$ was monitored over time. A plot of the natural logarithm of the simulated concentration of $E{\cdot}DNA_s$ versus time yields a pseudo first order rate constant that can be converted to k_{on} by dividing by the concentration of total enzyme in the simulation. The values of k_{off} were similarly determined by setting k_1 at zero and monitoring the disappearance of $E{\cdot}DNA_s$ over time. A plot of the natural logarithm of the simulated concentration of $E{\cdot}DNA_s$ versus time yields k_{off}. Initial fits of both k_{on} and k_{off} were determined by visually comparing simulation results with plots of $E{\cdot}DNA_s$ versus time. Surprisingly, curves corresponding to k_{on} were very close to the experimental values using the initial estimates of the microscopic rate constants. In contrast, large values of k_4 were required to fit the dissociation curve of the 14 bp substrate to the experimental value of k_{off}. Microscopic rate constants that had the largest impact on the generated curves were then determined. k_{off} responded most to changes in k_{-2} and k_4 while k_{on} was most greatly affected by k_{-1} and k_4. Changes in the scan length (resulting in changes in k_2, k_3, and k_{-3}) also affected both k_{off} and k_{on}. Simulated values of k_{on} and k_{off} were determined as described above for wide ranges of individual microscopic rate constants in order to determine the global value that fit the data with the smallest total percent deviation from all of the experimental results. Since no single solution was determined to be unique, small ranges for the microscoic rate constants were settled upon which resulted in no more than 15−20 percent deviation from the best fit to the experimental results. The final values of the individual rate

[2] The values of k_2 and k_3 both decrease with increasing length. In the limit in which these values become negligible, dissociation becomes dependent only upon k_{-2} and k_{-1}:

$$E{\cdot}DNA_s \xrightarrow{k_{-2}} E{\cdot}DNA_{ns} \xrightarrow{k_{-1}} E + DNA_{ns}$$

Since $k_{-1} \approx 8$ s^{-1} and the overall dissociation rate constant $k_{off} \approx 0.017$ s^{-1}, $k_{off} \approx k_{-2}$.

[3] The Gibbs free energy for nonspecific binding can be determined using the following equation:

$$\Delta G_{ns} = -RT \ln K_{ns} \quad (9)$$

The magnitude of the kinetic dissociation rate constant (in this case, k_4(can be determined by the activation energy required to reach the transition state between bound and free protein ($\Delta G^{\ddagger}$):

$$k_4 = \frac{kT}{h} \exp\left(-\frac{\Delta G^{\ddagger}}{RT}\right) \quad (10)$$

where k and h are the Boltzmann and Plank constants, respectively. The minimal value of $\Delta G^{\ddagger}$ is ΔG_{ns}, and any increase in $\Delta G^{\ddagger}$ results in a lower value of k_4.

constants can be seen in Table 2 and the simulated k_{on} and k_{off} data in Table 1. The best values of k_2, k_3, and k_{-3} correspond to an average scan length of 230−270 bp. Once the values of k_{on} and k_{off} were determined to our satisfaction, the results were checked by determining K_d by dividing k_{off} by k_{on}. The outcome of these calculations can be seen in Table 1. The values generated by the simulations are very similar to those determined experimentally, demonstrating that our proposed mechanism is consistent with our observations.

DISCUSSION

Structural and functional investigations of stable enzyme−DNA complexes have led to a detailed understanding of sequence-specific recognition and catalysis. However, intermediates involving protein−DNA interactions prior to the formation of a specific complex are critical to the recognition process (von Hippel, 1994). Changes in MTase efficiency resulting from increases in flanking DNA strongly implicate MTase−nonspecific DNA interactions in a facilitated diffusion mechanism (M. A. Surby and N. O. Reich, accompanying manuscript). The complexity of the kinetic steps that contribute to the catalytic constants k_{cat} and K_m, including specific site recognition, methyl transfer, and product dissociation, makes a detailed mechanistic interpretation of these results difficult. Therefore, to isolate the contributions of facilitated diffusion to initial site location and allow for direct comparisons with the other systems and models, we investigated the MTase's DNA length dependencies of K_d, k_{on}, and k_{off} under noncatalytic conditions.

The 20-fold increase in k_{on} with increasing DNA length shown in Table 1 is strong evidence for a facilitated diffusion mechanism. The large values of k_{on} are consistent with the diffusion controlled formation of a stable MTase−DNA complex and the DNA length dependency is that predicted by the theory of Berg et al. (1981). It should be noted that k_{on} is calculated from the ratio of k_{off} over K_d and that the observed changes are due to the relative independence of k_{off} to changes in DNA length and the twenty fold decrease in K_d with increasing DNA length shown in Table 1. Therefore, any molecular explanation for the trend observed for k_{on} must also be consistent with the trends for k_{off} and K_d. While the theory of Berg et al. (1981) is able to fit the k_{on} data using eq 3, it is insufficient to explain the trends in k_{off} and K_d as it predicts that k_{off} should increase 15-fold and K_d decrease only slightly as the DNA length is increased from 14 to 775 bp. Therefore, the model must be modified to account for the results presented in Table 1.

The relative independence of k_{off} and concomitant dependence of k_{on} to changes in DNA length might at first appear to be problematic; the reversible processes of association and dissociation should involve the same intermediates and transition states, according to the principle of microscopic reversibility. However, differences in the length dependent trends of k_{off} and k_{on} may be due to the fact that association via facilitated diffusion involves both three- and one-dimensional searches, while dissociation is limited to one-dimensional diffusion. The probability of encountering a DNA end is much greater during a one- rather than a three-dimensional process as long as the ends are at a distance less than the average scanning distance for the protein. Therefore, any impact end association may have on MTase binding is more likely to be manifested in k_{off} than in k_{on}. One probable result of encountering a DNA end would be destabilization due to rapid loss of binding contacts between the MTase and the DNA. The effects of destabilization would be most pronounced for short substrates, where the probability of diffusing to an end is the greatest. This could counteract the stabilization gained by short substrates through the increased probability of reassociation with the specific site during one-dimensional diffusion (Berg et al., 1981). The net result would be a k_{off} that is relatively independent of DNA length.

End dissociation is also supported by the changes observed for K_d (Table 1). The lowering of K_d with increasing DNA length must be due to stabilization of the bound MTase−DNA complex, since changes in K_d reflect changes in energy differences between bound and unbound states. Based upon the binding affinity of the MTase for nonspecific DNA, the addition of 760 nonspecific binding sites is predicted to reduce K_d for the 775 bp substrate only twofold when compared to the 14 bp substrate, suggesting that changes in K_d are not simply due to the presence of additional binding sites.[4] We suggest that increasing the length of nonspecific flanking DNA reduces the destabilizing effect deriving from DNA ends by lowering the probability that a DNA end will be encountered during dissociation.

In order to test whether dissociation via DNA ends would indeed result in the trends shown in Table 1, a computer simulation of Scheme 1 was run using the program, KINSIM (Barshop et al., 1983), which incorporated some of the microscopic rate constants which describe one-dimensional diffusion developed by Berg et al. (1981). As can be seen by the simulated results in Table 1, this kinetic mechanism is consistent with the experimental results. While some parameters had a greater effect on the outcome than others, changes in parameters tended to affect the values of k_{off} and k_{on} in an opposing manner. As an example, increasing the value of k_{-1} improved the fit of k_{off} while worsening the fit of k_{on}. Conversely, increasing k_2 (and therefore k_3 and k_{-3}, by definition) improved the fit of k_{on} and worsened the fit of k_{off}. These opposing changes allowed for a unique solution to be determined with only a minor degree of uncertainty in the final values of the individual microscopic rate constants, as represented by the range of values for these parameters listed in Table 2 which describe the best fit to the experimental data. We were also able to fit our experimental data to Scheme 1 with $k_{-3} = 0$, which assumes that dissociation is manditory once the end is reached. However, this mechanism excludes those enzymes which do not dissociate via the ends of the DNA and we felt that k_{-3} should remain in the model to make it more universally applicable. When the dissociation rate constant from the end

[4] If K_d represents the affinity of the MTase for the entire DNA molecule, then the apparent affinity could be represented by the sum of the equilibrium association constants for all possible binding sites, $K_{obs} = K_s + nK_{ns}$, where n is the number of nonspecific sites. K_s may be represented by $1/K_d$ of the 14 bp substrate and $K_{ns} = 1/K_d$ for a single nonspecific site. The resulting apparent K_d for the molecule as a whole would be 0.22 nM, since $K_d = 1/K_{obs}$ in this case. There is also a pseudosite (GAAATC) present in the 378 bp substrate and two pseudosites (GAAATC and GAATAC) in the 775 bp DNA. It is unlikely that they make a significant contribution since the K_d of the pseudosite is almost certainly less than either the K_d of the specific site or the sum K_d of the nonspecific sites on these two substrates (Reich et al., 1992). None of the smaller substrates contains pseudosites.

is considered to be equivalent to the dissociation rate constant from any nonspecific site ($k_4 = k_{-1}$), the changes in k_{off} and k_{on} with increasing DNA length are the same as the trends predicted by eqs 3 and 4 from the theory of Berg et al. (1981) (data not shown). Use of this method provides an alternative system for the quantitative analysis of facilitated diffusion and may assist in gaining insight into previously unknown phenomena, such as the end dissociation effect explored here.

The strongest evidence for the existence of an end effect is the slower dissociation rate for the MTase with a circular DNA molecule when compared to a linear substrate of equivalent length (Figure 4). Circularization of the linear substrate effectively removes the possibility of end destabilization from the kinetic scheme for dissociation. Thus, the kinetic scheme describing dissociation from the circular substrate is the two step process of Berg et al. (1981). The results with the linear substrate are consistent with the original results with the 378 bp substrate (Table 1). The k_{off} for circular DNA (0.006 s^{-1}) is very close to the value of 0.005 s^{-1} predicted by a simulation of Scheme 1 using the microscopic rate constants for the 378 bp DNA (Table 2) and setting k_3, k_{-3}, and k_4 equal to 0. Presumably, circularization removes the rapid dissociative pathway provided by end destabilization, and results in the MTase remaining associated with the molecule for a longer period of time. In an attempt to test whether a protein which does not conform to the theory of Berg et al. (1981) would show a lack of an end effect, these experiments were also performed using the *Eco*RI ENase. No significant difference in k_{off} from DNA that was either linear or circular was observed for the ENase (data not shown), supporting the prediction that this enzyme does not readily dissociate via DNA ends and could be modeled by Scheme 1 using $k_4 = k_{-1}$.

The results presented here parallel those determined under catalytic conditions (M. A. Surby and N. O. Reich, accompanying manuscript). Like the 8-fold difference in K_m (M. A. Surby and N. O. Reich, accompanying manuscript), the 20-fold decrease in K_d with increasing DNA length exceeds the changes predicted assuming a standard three dimensional search process by the MTase. Although a comparison of K_m and K_d is complicated by additional kinetic terms that may contribute to K_m, the fact that both decrease with increasing DNA length suggests that common kinetic steps strongly influence both parameters. Thus, the trend in K_m may be assumed to be due mostly to the enhancement of ternary complex formation and the stabilizing effect of removing the ends from the proximity of the specific site. Changes in k_{cat}/K_m are remarkably similar to k_{on} in actual value as well as length dependence. k_{cat}/K_m ranges from 0.24 $\times 10^8$ M^{-1} s^{-1} for a 14 bp long DNA to 1.0 $\times 10^8$ M^{-1} s^{-1} for 429 bp (M. A. Surby and N. O. Reich, accompanying manuscript), which is virtually identical to changes in k_{on} between the 14 bp and 378 bp substrates (Table 1). This suggests, as previously proposed on the basis of the large k_{cat}/K_m values (M. A. Surby and N. O. Reich, accompanying manuscript), that k_{on} determines k_{cat}/K_m and that the catalytic efficiency of the MTase is thus controlled by the rate of diffusion to the DNA substrate. The average scanning distance of the MTase determined here is also consistent with that suggested by the catalytic data. While the catalytic data could only imply a reasonable upper limit for this parameter (<400 bp), fitting the noncatalytic data to the model described by Scheme 1 confirmed this value and refined it to a range 230−270 bp. The enhancement in k_{cat}/K_m for larger DNA substrates illustrates the advantage gained by increasing the effective substrate target size 20−30-fold.

Since the MTase is part of a type II restriction modification system, it is of interest to compare the results here with those found previously with the *Eco*RI endonuclease (ENase). The k_{off} of the ENase increases 9-fold from 0.005 to 0.045 s^{-1} for a 34 bp and 4361 bp substrate, respectively (Jack et al., 1982), while K_d for the ENase is essentially identical for these two substrates (Terry et al., 1983). Both sets of data are consistent with the theory of Berg et al. (1981) and the values of k_{off} correspond to an average scanning distance of 1300 bp (Jack et al., 1982). This correlation with the predictions of Berg et al. (1981) suggests that the ENase most likely does not dissociate rapidly upon encountering the end of a DNA molecule. In addition, experimental results showed no significant difference between ENase dissociation from the linear and circular substrates (data not shown). The fact that the MTase is functional as a monomer while the ENase acts as a dimer may play a role in the differential stabilities of the two enzymes at DNA ends. For example, protein−protein interactions between the subunits that make up the ENase dimer could enhance stability by compensating for lost protein-DNA contacts. Furthermore, the MTase requires a cofactor for specific site binding. Loss of the cofactor upon encountering a DNA end could significantly reduce the binding affinity of the MTase for DNA, while no equivalent interaction exists for the ENase. In the preceding paper (M. A. Surby and N. O. Reich, accompanying manuscript), we discussed the contribution of facilitated diffusion to the effectiveness of the MTase and ENase in terms of host protection and viral restriction. It is possible that differential interactions with DNA ends may also contribute to the effectiveness of the two proteins in this regard. DNA end stability for the ENase is logical given that one of the few places where DNA ends might be encountered would be on invading phage DNA. Upon reaching the end of one of these molecules, the ENase will continue scanning for cleavage sites while the MTase will likely dissociate, giving the ENase another advantage in terms of restriction of viral DNA.

The study presented here and in the accompanying paper (M. A. Surby and N. O. Reich, accompanying manuscript) represent a comprehensive examination of the mechanism of specific site location by the MTase. The strength of examining the effects of length on both catalysis and binding is that the catalytic results describe the impact of facilitated diffusion on the efficiency of the MTase under standard reaction conditions while the binding results allow for an accurate quantitative determination of the parameters which describe facilitated diffusion by the MTase. The results presented here confirm the implications of the catalytic data and allow for the development of a novel addition to the kinetic scheme of facilitated diffusion. The method of modeling facilitated diffusion data described in this paper complements the theory of Berg et al. (1981) by allowing facile expansion of the ideas developed therein.

REFERENCES

Barshop, B. A., Wrenn, R. F., & Frieden, C. (1983) *Anal. Biochem. 130,* 134−145.

Berg, O. G., Winter, R. B., & von Hippel, P. H. (1981) *Biochemistry 20*, 6929−6948.
Becker, C. R., Efcavitch, J. W., Heiner, C. R., & Kaiser, N. F. (1985) *J. Chromatogr. 326*, 9293−9305.
Bloomfield, V. A., Crothers, D. M., & Tinoco, Jr., I. (1974) *Physical Chemistry of Nucleic Acids*, Chapter 5, Harper and Row, New York.
Brown, E. D., Marquardt, J. L., Lee, J. P., Walsh, C. T., & Anderson, K. S. (1994) *Biochemistry 33*, 10638−10645.
Dowd, D. R., & Lloyd, R. S. (1990) *J. Biol. Chem. 265*, 3424−3431.
Greene, P. J., Heynecker, H. L., Bolivar, F., Rodriquez, R. L., Betlach, M. C., Covarrubias, A. A., Bachman, K., Russel, D. J., Tait, R., & Boyer, H. W. (1978) *Nucleic Acids Res. 5*, 2373−2380.
Herendeen, D. R., Kassavetis, G. A., & Geidusschek, P. E. (1992) *Science 256*, 1298−1303.
Innis, M. A., & Gelfand, D. H. (1990) in *PCR Protocols: A Guide to Methods and Applications* (Innis, M. A., Gelfand, D. H., Sninsky, J. J., & White, T. J., Eds.) pp 3−12, Academic Press, San Diego, CA.
Jack, W. E., Terry, B. J., & Modrich, P. (1982) *Proc. Natl. Acad. Sci. U.S.A. 79*, 4010−4014.
Kati, W. M., Johnson, K. A., Jerva, L. F., & Anderson, K. S. (1992) *J. Biol. Chem. 267*, 25988−25997.
Moore, K. J. M., & Lohman, T. M. (1994) *Biochemistry 33*, 14565−14578.
Nardone, G., George, J., & Chirikjian, J. G. (1986) *J. Biol. Chem. 261*, 12128−12133.
Polesky, A. H., Dahlberg, M. E., Benkovic, S. J., & Grindley, N. D. F. (1992) *J. Biol. Chem. 267*, 8417−8428.
Reich, N. O., & Mashhoon, N. (1990) *J. Biol. Chem. 265*, 8966−8970.
Reich, N. O., Olsen, C., Osti, F., & Murphy, J. (1992) *J. Biol. Chem. 267*, 15802−15807.
Ricchetti, M., Metzger, W., & Heumann, H. (1988) *Proc. Natl. Acad. Sci. U.S.A. 85*, 4610−4614.
Riggs, A. D., Bourgeois, S., & Cohn, M. (1970) *J. Mol. Biol. 53*, 401−417.
Rubin, R. A., & Modrich, P. (1977) *J. Biol. Chem. 252*, 7265−7272.
Stowers, D. J., Keim, J. M. B., Paul, P. S., Lyoo, Y. S., Merion, M., & Benbow, R. M. (1988) *J. Chromatogr. 444*, 47−65.
Surby, M. A., & Reich, N. O. (1996) *Biochemistry 35*, 2201−2208.
Terry, B. J., Jack, W. E., Rubin, R. A., & Modrich, P. (1983) *J. Biol. Chem. 258*, 9820−9825.
van Zoelen, E. J. J. (1992) *Anal. Biochem. 200*, 393−399.
von Hippel, P. H. (1994) *Science 263*, 769−770.
von Hippel, P. H., & Berg, O. G. (1986) *Proc. Natl. Acad. Sci. U.S.A. 83*, 1608−1612.
von Hippel, P. H., & Berg, O. G. (1989) *J. Biol. Chem. 264*, 675−678.
Winter, R. B., & von Hippel, P. H. (1981) *Biochemistry 20*, 6948−6960.
Winter, R. B., Berg, O. G., & von Hippel, P. H. (1981) *Biochemistry 20*, 6961−6977.

BI951884F